The role of subunit cooperativity on ryanodine receptor 2 calcium signaling

D'Artagnan Greene, Tyler Luchko, Yohannes Shiferaw

Department of Physics & Astronomy, California State University, Northridge

Abstract

The ryanodine receptor type 2 (RyR2) is composed of four subunits which control calcium (Ca) release in cardiac cells. RyR2 serves primarily as a Ca sensor and can respond to rapid sub-millisecond pulses of Ca while remaining shut at resting concentrations. However, it is not known how the four subunits interact in order for the RyR2 to function as an effective Ca sensor. To address this question, and to understand the role of subunit cooperativity in Ca mediated signal transduction, we have developed a computational model of the ryanodine receptor 2 (RyR2) composed of four interacting subunits. We first analyze the statistical properties of a single RyR2 tetramer, where each subunit can exist in a closed or open conformation. Our findings indicate that the number of subunits in the open state is a crucial parameter that dictates RyR2 kinetics. We find that three or four open subunits are required for the RyR2 to harness cooperative interactions in order to respond to sub-millisecond changes in Ca, while at the same time remaining shut at the resting Ca levels in the cardiac cell. If the required number of open subunits is lowered to one or two, the RyR2 cannot serve as a robust Ca sensor, as the large cooperativity required to stabilize the closed state prevents channel activation. Using this 4-subunit model, we analyze the kinetics of Ca release from a RyR2 cluster. We show that the closure of a cluster of RyR2 channels is highly sensitive to the balance of cooperative interactions between closed and open subunits. Based on this result, we analyze how specific interactions between RyR2 subunits can induce persistent Ca leak from the sarcoplasmic reticulum (SR), which is believed to be arrhythmogenic. Thus, these results provide a framework to analyze how a pharmacologic or genetic modification of RyR2 subunit cooperativity can induce abnormal Ca cycling that can potentially lead to life-threatening arrhythmias.

Statement of significance

The ryanodine receptor type 2 (RyR2), which is composed of four interacting subunits, is the main channel responsible for calcium signal transduction in many cell types. However, it is not understood how the interaction between subunits determines the functionality of RyR2. In this study we show that subunit cooperativity is crucial in order for RyR2 to serve as an effective calcium sensor. We also show that small changes in subunit cooperativity can induce RyR2 leak, which is known to induce life-threatening cardiac arrhythmias.

Introduction

In cardiac cells, voltage sensitive ion channels in the cell membrane regulate processes within the cell by controlling the flow of ions between intracellular stores. The main ion responsible for signal transduction in the heart is calcium (Ca), which is stored at a high concentration in the sarcoplasmic reticulum (SR). By controlling the flow of Ca across the SR, the Ca concentration in the cell can be modulated in order to regulate an array of signaling cascades (1-3). An important protein that controls Ca release in cardiac myocytes is the Ryanodine Receptor Type 2 (RyR2). Cryo-EM studies reveal that the RyR2 is composed of 4 identical subunits that control the diameter of a central pore (4, 5). These subunits are regulated by Ca binding to regulatory sites, which control the conformational state of the subunit. On a larger scale, RyR2 channels aggregate on the SR membrane to form tightly knit clusters of roughly 10-100 channels(6, 7). These clusters form synapse-like protrusions of the SR called junctional-SR (JSR) which are positioned close to voltage sensitive L-type Ca channels (LCCs) in the cell membrane. Signaling between the LCC and the RyR2 occurs in the restricted volume between these channels, which is referred to as the dyadic junction. During an action potential (AP), a small amount of Ca is released by the local LCCs into the dyadic junction. This Ca then binds to the local RyR2s, which leads to an increase in the open probability of the RyR2 channels, and subsequently, to a large flow of additional Ca into the dyadic junction from the SR. The additional Ca released is localized in the vicinity of the RyR2 cluster and is referred to as a Ca spark. Using this approach, membrane currents can excite sparks that are spatially distributed in the cell, in order to activate a wide range of intracellular processes.

In the cardiac cell, the main function of a single RyR2 channel, and clusters of RyR2 channels, is to serve as a robust Ca sensor. LCCs typically have a mean open time in the sub-millisecond range, so that a crucial design feature of the RyR2 is that it must have the capacity to respond to changes in Ca concentration on this time scale (8). A second design feature of the RyR2 is that it must reliably shut at the resting Ca concentration in the cardiac cell ($\sim 0.1\ \mu M$). This feature determines the stability of Ca release from the SR, and it is crucial to maintaining normal Ca cycling homeostasis in the cell. There are now many studies that have shown that various disease states are associated with abnormal Ca release from the SR, which has been attributed to leaky RyR2 channels (9-11). However, how the RyR2 can respond rapidly to sub-millisecond pulses of Ca, and at the same time remain stable at the resting Ca concentration, is not completely understood. Previous studies have argued that this capacity of RyR2 is achieved due to the high nonlinearity of the channel response, which arises from cooperative interactions between subunits and neighboring RyR2s (12-15). However, it is not understood how specific interactions between subunits regulate the nonlinear response of RyR2.

In this study, we analyze the statistical properties of a single RyR2 channel composed of four interacting subunits and clusters of RyR2 channels. Our goal is to determine how cooperative interactions between subunits dictate the capacity of the RyR2 to serve as a robust Ca sensor. To address this question, we first analyze the statistical properties

of a single RyR2 channel where each subunit can be either in the closed or open state. In this case we show that RyR2 cooperativity is dictated by two dimensionless parameters, denoted by δ and ϵ, which represents the energy penalty to introduce a conformational mismatch between two adjacent closed and open subunits, respectively. Using this approach, we show how subunit-subunit interaction energies allow RyR2 to respond rapidly to sub-millisecond changes in the local Ca concentration while remaining stably shut at the resting Ca levels in the cardiac cell. Our main finding is that a crucial parameter that dictates the function of RyR2 is the number of subunits that are required to be in the open state for the channel as a whole to open and permit Ca flow. In this regard, we find that if the number of subunits that are required to be in the open state is three or four, there is a broad region in parameter space where RyR2 is an effective Ca sensor. However, if only one or two subunits are sufficient, we find that system parameters must be finely tuned for RyR2 to function effectively. Thus, our results predict that to optimize Ca signaling fidelity, RyR2 only allows Ca across the pore when three to four subunits are in the open state. A second finding in this study is that strong subunit cooperativity can make RyR2 more responsive to changes in Ca in the dyadic junction, while at the same time stabilizing the closed state of the channel at the resting Ca concentration. However, we find that this effect only occurs when δ and ϵ are tuned to a restricted region in parameter space. Thus, cooperativity improves the capacity of RyR2 to serve as a Ca sensor provided that key energetic constraints are satisfied. We have also studied the response of a cluster of RyR2 channels to sub-millisecond changes in local Ca levels. In this case, we again find that δ and ϵ must be tuned to a restricted region in parameter space for a Ca spark to both form and be reliably extinguished. Outside of this region, we show that Ca sparks are long-lasting, or alternatively, that Ca sparks cannot be activated by a physiologically relevant Ca pulse in the vicinity of the RyR2 cluster. These findings suggest that Ca leak from the SR, which is known to be arrhythmogenic, is sensitive to the delicate balance of subunit-subunit interactions which stabilize the closed and open state of the RyR2.

Methods

Model of a single RyR2 subunit

Cryo-EM studies reveal that the RyR2 is composed of four identical subunits that control the diameter of a central pore (5, 16-18), as shown in Figure 1A. Each subunit potentially has several Ca binding sites, which can regulate the conformation of the RyR2. From an analysis of the cryo-EM structures, a single activating Ca binding site on each subunit has been identified on the cytosolic side of the channel (5, 19). It is generally believed that once Ca binds to the activating Ca binding site, allosteric interactions induce the pore lining S6 segment to tilt away from the central axis, increasing the diameter of the pore(4). To model RyR2, we will first assume that each subunit can be in a closed (0) or open (1) conformation. Transitions between these states will obey the reaction scheme

$$0 \underset{k_{10}}{\overset{k_{01}}{\rightleftharpoons}} 1 \quad , \tag{1}$$

where k_{01} is a Ca dependent forward rate, and k_{10} is the closing rate. In a previous study (20), we developed a more complex gating scheme with an additional closed state which was introduced to model RyR2 flickering observed at

concentrations above $\sim 10\mu M$ (21). In this study, we have opted for a minimal two state model given the paucity of experimental data needed to constrain the interactions between these states. Following our previous study, we note that the closed to open transition will be regulated by a single Ca binding site, which we take to be the activating Ca binding site. Thus, the open rate will obey first order kinetics and have the form

$$k_{01} = A_{01}\frac{[Ca]}{[Ca] + c_{th}} \tag{2}$$

where $[Ca]$ denotes the concentration of Ca on the cytosolic side of the RyR2. Here, c_{th} is the half-maximal concentration constant for Ca binding, and A_{01} is the maximal binding rate at high Ca concentrations $[Ca] \gg c_{th}$. The choice of parameters A_{01} and c_{th} will be constrained by experimental measurements of the RyR2 in lipid bilayers and will be discussed in a following section.

Modeling the effect of subunit-subunit interactions

Equilibrium properties of the RyR2 tetramer. The goal of this paper is to understand how interactions between RyR2 subunits determine the properties of the channel as a whole. Analysis of the cryo-EM structure of the RyR2 reveals that adjacent subunits interact, but there are few, if any, interactions between diagonal subunits. This can be seen qualitatively in the cryo-EM structure of the closed state of the RyR2 in Figure 1A. Figure 1Aii presents a top-down view from the cytosolic side of the closed RyR2 channel. We note in Figure 1Aii that any given subunit is in direct contact with a subunit directly adjacent to it on either side, but it is not in direct contact with the subunit diagonally across from it. Figure 1Aiii presents a top-down view from the luminal side showing that there are direct contacts between adjacent subunits but not between diagonal subunits. We can make these observations quantitative by using UCSF Chimera X (22), a program for visualization and analysis of protein structure files, to identify the hydrogen bonds (H-bonds) between any two different subunits in the cryo-EM structure. Figure 1B shows that several H-bonds were identified between adjacent subunits in both the closed (PDB ID: 6JI8) and open (PDB ID: 6JIY) states of the channel while none were identified between subunits that were positioned directly across from each other. Hence, these results suggest that we use a nearest-neighbor interaction model where interactions between adjacent subunits are included in the model but interactions between diagonal subunits are not included.

To analyze the statistical properties of the RyR2 tetramer, we label conformations as a string of four numbers $\vec{s} = \{s_1, s_2, s_3, s_4\}$, where subunit i can be in the state s_i, which can be either 0 or 1. To compute the energy of the system, we first define the energy of a subunit in isolation in the closed and open state as $E[0]$ and $E[1]$, respectively. To account for the subunit-subunit interactions, we will incorporate only nearest-neighbor interactions between subunits s_i and s_{i+1}, as our foregoing analysis indicates that subunits s_i and s_{i+2} do not interact. Thus, we will introduce an interaction energy between adjacent subunits denoted as $E[s_i, s_{i+1}]$. Thus, there are 3 distinct interaction energies between subunits denoted as $E[1,1], E[0,0],\ E[0,1] = E[1,0]$. The total energy of a conformation $\vec{s}$ is then given by

$$E[\vec{s}] = \sum_{i=1}^{4} E[s_i] + E[s_i, s_{i+1}] \ , \tag{3}$$

where the cyclic geometry of the tetramer imposes periodic boundary conditions so that $s_5 = s_1$. Once these energies are defined, we can then compute the equilibrium properties of the system by computing the partition function

$$Z = \sum_{\{\vec{s}\}} \exp(-\beta \, E[\vec{s}]) \ , \tag{4}$$

where the summation is overall all possible conformations $\vec{s}$. In Appendix A, we give a full analysis of the partition function of the system.

Dynamics of the RyR2 tetramer. To model the dynamics of the RyR2, we will consider the stochastic dynamics between conformational states of the tetramer. To implement this, we will denote $K[\vec{s} \to \vec{u}]$ to be the transition rate from conformation $\vec{s}$ to $\vec{u}$, so that in a time step Δt the probability of that transition is given by $K[\vec{s} \to \vec{u}]\Delta t$. While the detailed kinetic parameters are not known, transition rates must satisfy the principle of detailed balance. This condition reads

$$\frac{K[\vec{s} \to \vec{u}]}{K[\vec{u} \to \vec{s}]} = \exp\big(-\beta\big[E[\vec{u}] - E[\vec{s}]\big]\big) \ . \tag{5}$$

To implement detailed balance, we will first consider the transition rate of subunit i from the closed to open conformation. This rate is taken to be

$$K_i[0 \to 1] = k_{01} \exp\left(-\frac{\beta \Delta E_i^{01}}{2}\right), \tag{6}$$

where

$$\Delta E_i^{01} = E[1, s_{i-1}] + E[1, s_{i+1}] \ - (E[0, s_{i-1}] + E[0, s_{i+1}]) \, , \tag{7}$$

which is the change in subunit-subunit interaction energy between the initial and final conformation. Similarly, the transition rate from the open state to the closed state is given by

$$K_i[1 \to 0] = k_{10} \exp\left(-\frac{\beta \Delta E_i^{10}}{2}\right), \tag{8}$$

where

$$\Delta E_i^{10} = E[0, s_{i+1}] + E[0, s_{i-1}] \ - (E[1, s_{i+1}] + E[1, s_{i-1}]) \ . \tag{9}$$

Note that we have included a factor of $1/2$ in the exponential so that forward and backward rates are treated on equal footing while satisfying detailed balance. Also, the energetic contributions due to the isolated subunit is accounted for by the rates k_{01} and k_{10}, since $k_{01}/k_{10} = \exp\big(-\beta(E[1] - E[0])\big)$.

The transition rates can be more succinctly expressed by introducing the matrix

$$Q\big[s_i, s_j\big] = \frac{\beta}{2}\Big[E\big[s_i, s_j\big] - E\big[1 - s_i, s_j\big]\Big], \tag{10}$$

so that

$$K_i[0 \to 1] = k_{01} \exp\left[Q[0, s_{i-1}] + Q[0, s_{i+1}]\right] , \quad (11)$$

$$K_i[1 \to 0] = k_{10} \exp\left[Q[1, s_{i-1}] + Q[1, s_{i+1}]\right] . \quad (12)$$

The matrix elements are

$$Q[0,1] = \epsilon, \quad (13)$$
$$Q[1,0] = \delta, \quad (14)$$
$$Q[0,0] = -\delta, \quad (15)$$
$$Q[1,1] = -\epsilon, \quad (16)$$

where

$$\delta = \left(\frac{\beta}{2}\right)(E[0,1] - E[0,0]), \quad (17)$$

$$\epsilon = \left(\frac{\beta}{2}\right)(E[0,1] - E[1,1]) . \quad (18)$$

Here, we note that ϵ and δ are dimensionless quantities which specify the energetic cost of introducing a mismatch between two adjacent subunits in the closed and open conformations, respectively.

Single channel simulation protocol. To time evolve the RyR2 tetramer from time t to $t + \Delta t$, the transition rate will be computed using the conformation at time t, and each subunit will be updated simultaneously at each time step. In particular, subunit i in state s_i at time t will transition to state $1 - s_i$ at time $t + \Delta t$ with probability $K_i[s_i \to 1 - s_i]\Delta t$, or remain in state s_i otherwise. To compute the open probability of the RyR2, denoted here as P_o, we simulate a single RyR2 for $t = 10^6\ ms$ using a time step $\Delta t = 0.005\ ms$. During this simulation, the total time spent in the open (T_o) and closed state (T_c) is computed, and these times are used to compute $P_o = T_o/(T_o + T_c)$, and the mean open and closed times. Similarly, the mean closed time is found by $\tau_c = T_c/n_c$, where n_c is the total number of times the RyR2 closes. This simulation is conducted for a range of cytosolic Ca concentrations in order to compute the Ca dependence of these quantities. In all simulations quantities are computed by averaging over 500 independent runs, and the error is estimated as the standard deviation.

Model parameters. To constrain model parameters, we will rely on measurements of single RyR2 kinetics in lipid bilayers by Xu and Meissner (23). In that study, the authors measured Ca ion flow across the pore in order to characterize the gating kinetics of the full RyR2. It should be noted that in these experiments the kinetics of individual subunits was not measured, so it is not known how many subunits are required to open to allow Ca ion flow. In particular, they measured P_o, and showed that the threshold for channel opening occurs at concentrations ~ 10 μM, so that we can take $c_{th} = 10$ μM. This choice is consistent with several studies which show that P_o increases rapidly with Ca around these concentration levels (21, 24). They also measured the average closed time of the RyR2 and found that it varied substantially with the Ca concentration. At resting concentration levels, $[Ca] \sim 0.1$ μM, they found that $\tau_c \sim 5000$ ms, which drops down to ~ 150 ms at $[Ca] \sim 1$ μM, and then further to ~ 1 ms for $[Ca] > 10$ μM. Note that for a high concentration, where $[Ca] > c_{th}$, the Ca dependence of binding is saturated, so that a

single subunit in the closed state will transition to the open state with a rate that is roughly A_{01}. Now, if $k_o = 1$, then the mean closed time is determined by the transition rate for one of the four closed subunits to open, which gives $\tau_c \sim 1/(4A_{01})$, so that we can estimate $A_{01} \sim 0.25\ (ms)^{-1}$. However, if $k_o > 1$ then τ_c will be larger and sensitive to the degree of cooperative interactions between subunits. Thus, given that we do not know the interaction strengths δ and ϵ, a reasonable choice of parameters is to simply take $A_{01} \sim 1\ (ms)^{-1}$. Finally, Xu and Meisner measured the mean open time (τ_o) of the channel and found that it increased moderately from ~ 0.5 ms at 0.1 μM to ~ 2 ms at 100 μM. In this case, the Ca dependence is weaker, and given that we do not know the parameters k_o, ϵ and δ, a reasonable choice of the single subunit closing rate is $k_{10} \sim 1\ (\text{ms})^{-1}$. In Table 1 we summarize the model parameters that we have used to characterize the RyR2.

The dynamics of a RyR2 cluster. In a cardiac cell, RyR2s are arranged in clusters that are distributed within the cell. Therefore, it is important to explore the role of subunit-subunit cooperativity in the signaling fidelity and stability of RyR2 clusters. To explore this feature, we will apply a spatially distributed cell model of intracellular Ca(25, 26). In this approach, the cell interior is divided into compartments that contain the key Ca cycling ion channels (see Figure 1C). The basic unit of the model is referred to as a Ca release unit (CRU), which is composed of the main compartments that surround a RyR2 cluster in the cell. The intracellular compartments that comprise the junctional CRU are: (1) The dyadic junctional space with concentration denoted as c_p^{ijk}, where ijk denotes the location of that CRU in a 3D grid representing the cell. This compartment represents the volume of the cell that is in the immediate vicinity of the local RyR cluster, which is roughly a pillbox of height $10nm$ and diameter $100nm$; (2) The submembrane space, with concentration c_s^{ijk}, which represents a volume of space in the vicinity of the dyadic junction. This space is larger than the dyadic junction, but much smaller than the local bulk cytosol; (3) The cytosol, with concentration c_i^{ijk}, which characterizes the volume of space into which Ca diffuses before being pumped back into the SR via the Sarcoplasmic-Endoplasmic Reticulum Calcium ATPase (SERCA) transporter; (4) The junctional sarcoplasmic reticulum (JSR), with concentration c_{jsr}^{ijk}, which is a protruding synapse-like section of the SR network in which the RyR2 channels are embedded; (5) The network SR (NSR), with concentration c_{nsr}^{ijk}, which represents the bulk SR network that is spatially distributed in the cell. In this study, we are interested in the dynamics of only a single RyR2 cluster. Thus, we will simulate only a small $5 \times 5 \times 5$ lattice of CRUs, and place an active RyR2 cluster at the 3,3,3 site, while all other fluxes in the cell are set to zero, and we will analyze clusters of 40 RyR2 channels which will be stimulated by a $1ms$ stimulus of varying amplitude. Following our previous study (20), luminal dependence of RyR2 is implemented by introducing a JSR load dependence of the RyR2 subunit opening rate. Thus, the forward rate given by Eq. 2 will be multiplied by a factor $\Phi(c_{jsr}) = 1/\left(1 + \left(c^*/c_{jsr}\right)^{\gamma}\right)$, where $\gamma = 5$, $c^* = 700$ μM, and where c_{jsr} denotes the JSR Ca concentration. This factor ensures that Ca sparks will terminate reliably since the forward rate k_{01} decreases rapidly as the JSR concentration is depleted. Also, rapid diffusion of $[Ca]$ away

from the dyadic space provides a strong negative feedback mechanism that promotes Ca spark closure. Here, we note that while this formulation provides a robust mechanism for Ca spark termination, alternative mechanisms have been proposed(27-29), and there is still no established mechanism that has been rigorously confirmed (2). In the discussion section we argue that the main results in this study should be independent of the detailed mechanism of Ca spark termination. All computational code developed in this study will be provided by the authors upon request.

Results

Dependence of RyR2 kinetics on subunit-subunit interactions

In this section, we will explore the role of subunit-subunit interactions on the gating kinetics of the RyR2. We first note that the opening of the pore will require a subset of the four subunits to be in the open conformation. Since this number is not known, we will define a variable $k_o = \{1,2,3,4\}$, so that if the number of subunits in the open conformation, denoted as k, satisfies the condition $k \geq k_o$, we will consider the RyR2 to be in the open state. For a given k_o, we will analyze single channel properties that govern the capacity of the RyR2 to serve as an effective Ca sensor.

The case $k_o = 4$.

As a starting point, we will first analyze the case where the RyR2 pore opens only when all four subunits are in the open state. Here, we will first consider the case of symmetric interactions, $\delta = \epsilon$, in order to assess how the open probability P_o depends on the strength of cooperativity. In Figure 2A, we plot P_o vs. $\log[Ca]$ for a range of subunit-subunit interaction strengths. This result shows that P_o has a sigmoidal dependence on $\log[Ca]$, and both the steepness and maximum P_o are increased with stronger subunit-subunit interactions. To understand the response properties of the RyR2, we can apply an exact solution for P_o for the $k_o = 4$ case, which is given in Equation B7 (Appendix B). Using this expression, we can set $\delta = \epsilon$ and evaluate P_o in the limit of strong and weak cooperativity. In the limit of weak cooperativity ($\delta \ll 1$), we find that $P_o \sim (\lambda/(\lambda+1))^4$, where $\lambda = k_{01}/k_{10}$, which is due to the requirement that all subunits must transition to the open state independently. At a high Ca concentration, which is induced by a local LCC opening where $[Ca] \gg c_{th}$, this gives $P_o \sim 0.2$. On the other hand, for high cooperativity ($\delta \gg 1$), we find that $P_o \sim \lambda^4/(\lambda^4+1) \sim 0.94$. Thus, at high $[Ca]$, strong coupling between subunits forces all of the subunits to the open state. Now, at resting concentrations ($[Ca] \sim 0.1$ μM) we find that $P_o \sim \lambda^4 \sim 10^{-7}$ for both strong and weak cooperativity. For the case $k_o = 4$, this result demonstrates that the RyR2 is reliably shut at low Ca concentrations independent of subunit-subunit interactions, but cooperativity can substantially improve the channel response at large Ca.

To determine the regime in parameter space where RyR2 exhibits closure at low Ca and opening at high Ca, we will vary both δ and ϵ. Thus, we will evaluate P_o at the resting Ca levels in the cell ($[Ca] \sim 0.1$ μM), which we will refer to as "low" Ca. Similarly, we will evaluate P_o at a "high" Ca concentration, which is present in the dyadic junction

during an LCC opening. In this latter case, the LCC should raise the local Ca concentration above the threshold of $c_{th} = 10$ μM, and we will assume that $[Ca] \gg c_{th}$. Thus, we will evaluate P_o at a "high" concentration, which we have chosen to be $[Ca] = 100\mu M$. We will denote all quantities evaluated at these low/high Ca concentrations using a superscript $-/+$. To define a RyR2 channel, which is reliably shut at low Ca, we will again refer to the experiments of Xu and Meissner (23), who estimated that $P_o \sim 10^{-4}$ at $\sim 0.1\mu M$. Thus, we will demarcate the region in parameter space where RyR2 is reliably shut using the condition $P_o^- \leq 10^{-4}$. Also, Xu and Meissner measured the RyR2 P_o at $[Ca] \sim 100\mu M$ and found it to be in the range $0.5 - 0.7$. Thus, we will demarcate the region of parameter space where the RyR2 responds effectively to high Ca using the condition $P_o^+ \geq 0.7$. Note that this choice is simply to demarcate visually the regime of high open probability and does not impact the subsequent conclusions. In Figure 2B we show the region in parameter space where $P_o^- \leq 10^{-4}$ and $P_o^+ \geq 0.7$. This result indicates that the relative strength of ϵ and δ is crucial for RyR2 to serve as an effective Ca sensor. The position of the $P_o^- = 10^{-4}$ line shown in Figure 2B indicates that RyR2 is reliably stable for a wide range of parameters (below the blue line). However, only a subset of this region (above the red line) will also satisfy $P_o^+ \geq 0.7$. For example, if $\delta = 0.5$, then RyR2 is an effective sensor only in the range $\epsilon \gtrsim 0.5$ and $\epsilon \lesssim 1$. Thus, there is a restricted region in parameter space where RyR2 is both reliably shut at low Ca while remaining responsive to sub-millisecond changes in the local Ca concentration.

In the cardiac cell, RyR2 are activated by LCC openings that raise the local Ca concentration for a duration $\lesssim 1ms$. Thus, at these transient concentration levels, RyR2 must transition from a closed to open conformation within a duration that is comparable or less than the mean LCC open time. If this condition is not met, the RyR2 cannot respond to the fast changes in local Ca required for signal transduction. A requirement for this property is that the mean closed time of RyR2, denoted as τ_c, must satisfy $\tau_c \lesssim 1ms$. Furthermore, for the RyR2 to be reliably shut under resting conditions, we expect τ_c to be substantially larger at baseline Ca concentration levels. In Figure 2C we plot $\log(\tau_c)$ as a function of $\log[Ca]$ for the case of symmetric interactions $\delta = \epsilon$. Here, we observe that in the case $\delta = 1.2$, τ_c^+ is the smallest of the 3 cases, while τ_c^- is the largest. This result indicates that cooperativity improves the capacity of the RyR2 to serve as an effective Ca sensor by reducing the response time while at the same time increasing stability. In order to gain insight about this behavior, we rely on our exact solution for τ_c given in Eq. C5 (Appendix C). In the limit of small $[Ca]$, and where we set $\delta = \epsilon$, we find that the leading order behavior is given by $\tau_c^- \propto \exp(2\delta)/[Ca]^4$ (see Eq. C6 for the case $\epsilon \neq \delta$). This expression indicates that at resting Ca levels, the mean closed time increases exponentially with δ. On the other hand, at high Ca, we find that $\tau_c^+ \propto \exp(-2\epsilon)$, which indicates that cooperativity decreases the mean closed time and therefore makes RyR2 more responsive to changes in Ca. This result indicates that cooperativity indeed makes RyR2 a more effective Ca sensor. However, this effect only applies as long as the leading order behavior, for low Ca, is governed by the term proportional to λ^{-1} in the full analytic expression (Eq. (C5)). A more detailed analysis for the parameters used in this study requires $\delta <$

$\epsilon + 0.4$ (Appendix C). If this inequality is violated, τ_c begins to grow exponentially with δ, and the stability of the closed state prevents sub-millisecond changes in Ca from inducing a RyR2 opening.

In order to capture the average closed time in the full $\delta - \epsilon$ plane, in Figure 2D we show the region in parameter space such that $\tau_c^+ \leq 1$ ms and $\tau_c^- \geq 5000$ ms. We have picked this condition since LCCs open for a duration of roughly $\sim 1ms$, and Xu and Meissner have measured $\tau_c \sim 5000$ ms at $[Ca] = 0.1$ μM. Thus, this condition demarcates the region in parameter space where the RyR2 is responsive to sub-millisecond changes in $[Ca]$ and where closed times are much longer than the pacing period.

The cases $k_o = 3$ and $k_o = 2$

In Figures 3 and 4, we plot the open probability and the mean closed time for the cases $k_o = 3$ and $k_o = 2$, along with the region in parameter space where $P_o^- \leq 10^{-4}$ and $P_o^+ \geq 0.7$, and where $\tau_c^+ \leq 1$ ms and $\tau_c^- \geq 5000$ ms. For the case $k_o = 3$, we find that there is a broad regime of parameter space where RyR2 is an effective Ca sensor. On the other hand, for $k_o = 2$, the effective regime shrinks substantially. In this case, we find that only in a very restricted parameter regime can RyR2 serve as an effective Ca sensor.

The case $k_o = 1$

For the case $k_o = 1$ we found that, for the parameters used in this study (Table 1), it is not possible to construct an effective RyR2 sensor. This result can be understood using the exact solution for P_o and τ_c for the case $k_o = 1$ (Appendix C). In particular, we note that at low Ca we have that $\lambda \sim 0.02$, so that Eq. B10 will be dominated by the lowest order term in λ, which gives $P_o^- \sim 4\gamma^2\lambda = 4\exp(-4\delta)\lambda$. In addition, the condition that $P_o^- \leq 10^{-4}$ requires that $\delta \geq 1.7$. Thus, strong cooperativity is required to stabilize the closed channel, since in this case only one subunit is required to transition to the open state for the whole channel to open. However, the mean closed time in this case is simply $\tau_c = (1/4k_{01})\exp(2\delta)$. If we require that $\tau_c \leq 1$ ms, we have the constraint $\delta \leq 0.5$, which is incompatible with the requirement that $P_o^- \leq 10^{-4}$. Thus, when $k_o = 1$, the RyR2 cannot be reliably shut at low Ca while also responding readily to the rapid changes in Ca in the dyadic junction. Thus, the RyR2 cannot serve as a reliable Ca sensor if only one subunit determines channel opening.

Signaling and stability of a Ca spark

In the cardiac cell, RyR2 channels aggregate into clusters which release Ca in the form of discrete events called Ca sparks. However, it is not understood how cooperative interactions between RyR2 subunits can modify the flux of Ca that underlies a Ca spark. To model a RyR2 cluster, we apply the 3D computational cell model described previously (20). In Figure 5A, we show the local dyadic junction concentration c_p, the local JSR load c_{jsr}, and the number of open channels in the cluster n_o. In this simulation, a stimulus current is applied at time $t = 20$ ms in the vicinity of a RyR2 cluster of 40 channels. The initial SR load is taken to be $1400\mu M$, which is larger than the normal

steady state value of $\sim 1000\mu M$, in order to probe the regime of high excitability where Ca cycling abnormalities are expected to develop. The increase in Ca due to the stimulus ignites a Ca spark, where the dyadic junction concentration rises to $c_p \sim 300$ μM and then decays to baseline (~ 0.1 μM). During this time, the JSR load is depleted from the resting SR load, and then recovers as the JSR is refilled (Figure 5B) by the sarcoplasmic reticulum calcium ATPase (SERCA) pumps. In Figure 5C we show the number of open RyR2 channels as a function of time. Figure 5C shows that, during a Ca spark, most of the 40 RyR2 channels in the cluster open and then are gradually closed.

To explore the role of subunit-subunit interactions on spark kinetics, in Figure 5E we show c_p as a function of time for a range of δ values. In this simulation, we have fixed $\epsilon = 0.8$ and consider the cases $\delta = 0.2, 0.8,$ and 1.6. For $\delta = 0.2$, we find that c_p peaks at $c_p \sim 400$ μM, and then proceeds to decay and fluctuate around $c_p \sim 50$ μM. As coupling is increased to $\delta = 0.8$, we find that c_p peaks at $c_p \sim 300\mu M$, and then the Ca concentration decays to the resting level of $c_p \sim 0.1\mu M$. Finally, for $\delta = 1.6$, we find that the trigger current does not excite a Ca spark during the full-time interval simulated. To gain more insight into the dynamics that underlie the Ca transient, in Figure 5F we have plotted the number of open channels n_o as a function of time. Our results show that for $\delta = 0.2$, the cluster does not shut properly as there are still roughly ~ 10 channels open during the steady state at the end of the simulation. Consequently, the JSR does not refill since the cluster never shuts (Figure 5G). This phenomenon is well known, both in computational studies and experimentally, and is referred to as a long-lasting spark(2, 15, 30, 31). In this case, the shut cluster is unstable, as random RyR2 openings promote a sustained Ca flux from the SR. Now, for $\delta = 0.8$, we find that indeed n_o rises to a full cluster opening with $n_o \sim 40$, and then proceeds to close and shut with $n_o = 0$ approximately half way through the simulation. Finally, in the case $\delta = 1.6$, we find that the RyR2 cluster remains shut throughout since the stimulus was not sufficient to overcome the energy penalty for cluster opening.

To capture the dynamics of the system, we will determine the regions in the $\delta - \epsilon$ parameter space where normal sparks, long-lasting sparks, and spark activation failure occur. To identify these regions, we will inject a $1ms$ current pulse in the dyadic junction at time $t = 0$ to activate the local RyR2 cluster. In this case, we have chosen the amplitude of the stimulus to be $150\mu M/ms$, which raises the local concentration above threshold ($\sim 30\mu M$). To keep track of the RyR2 response to the pulse, we measure the number of open RyR2 channels n_o, and count spark activation when $n_o > 5$. Once the spark is activated, we then determine the time τ_s until it has extinguished when $n_o = 0$. In this manner we distinguish three distinct cases: (i) Failure to activate when $\tau_s < 10ms$, (ii) Normal sparks with $10ms < \tau_s < 100ms$, and (iii) Long-lasting sparks $\tau_s > 100ms$. In Figure 6A-C, we show the phase diagram of the system for $k_o = 4, 3,$ and 2. Here, the key finding is that normal Ca sparks occur only in a restricted region of parameter space. In particular, we find that by increasing ϵ, a normal spark will transition to a long-lasting spark.

Similarly, increasing δ leads to spark activation failure. Thus, a normal Ca spark response occurs only within a limited region of parameter space.

For the case $k_o = 1$, we found that Ca sparks, when activated, always evolved to a long-lasting spark. In Figure 7A, we show c_p for both weak ($\delta = 0.2$) and strong ($\delta = 1.2$) cooperativity. In both cases, we find that once a spark is activated, the diastolic Ca never decays to baseline. In Figure 7B we show n_o, which indicates that at steady state the RyR2 cluster is never completely shut. This result, which is consistent with our single RyR2 analysis, shows that the RyR2 cannot serve as an effective Ca sensor if only one subunit needs to transition to the open state to open the channel.

Spontaneous Ca sparks

In the absence of an external trigger, Ca sparks can occur due to random fluctuations in the RyR2. These sparks are referred to as spontaneous Ca sparks, since they are not induced by an external Ca flux. In this section, we analyze the dependence of the timing of spontaneous Ca sparks on RyR2 subunit-subunit interactions. In Figure 8A, we simulate a cluster of 40 RyR2 channels for a long duration of $t = 1500ms$. In this case, the stimulus current is not activated, so that the two Ca sparks that occur are spontaneous. To ensure that the spontaneous Ca sparks are not activated by random LCC openings, we have set the LCC conductance to zero. To characterize the timing of spontaneous Ca sparks, we measure the waiting time T_s, as indicated in Figure 8A, to the first spontaneous Ca spark, and then compute the average $\langle T_s \rangle$ using 500 independent simulation runs. In Figure 8B, we plot $\langle T_s \rangle$ vs δ for $\epsilon = 0, 0.5,$ and 1.0 showing that $\langle T_s \rangle$ is highly sensitive to δ. In Figure 8C, we plot the line $\langle T_s \rangle = 400ms$ in the $\delta - \epsilon$ parameter space for the cases $k_o = 4, 3,$ and 2. Here, the left/right side of the line denotes the region where $\langle T_s \rangle < 400ms$ and $\langle T_s \rangle > 400ms$ respectively. As the number of open subunits k_o is decreased, we see that the boundary shifts right, indicating that the cluster is more unstable to spontaneous Ca sparks that occur with a frequency less than $400ms$. These results indicate once again that the timing of spontaneous Ca sparks is highly sensitive to the balance between the energy penalties δ and ϵ.

Discussion

The requirements for RyR2 to serve as an effective Ca sensor. In this study, we have highlighted the key requirements in order for the RyR2 to serve as an effective Ca sensor. The first crucial requirement is that the RyR2 must transition to the open state in response to the Ca concentration changes invoked by the LCC. On the other hand, when the concentration of Ca is such that the channel is in the resting state, RyR2 channels must remain shut. This requirement is crucial, since Ca regulates a wide range of subcellular processes which will be disrupted by uncontrolled Ca release from the SR. A key finding in this study is that k_o, which is the number of subunits which must be in the open state in order for the RyR2 pore to open, determines whether or not the RyR2 operates as an

effective Ca sensor. For the case $k_o = 4$, we found that at low $[Ca]$, even in the absence of cooperativity, the RyR2 can remain shut for long durations. This is because the probability that all four subunits transition to the open state scales as $\lambda^4 \sim [Ca]^4$, which is small at the resting Ca concentration of $\sim 0.1\mu M$. However, at high Ca, the open probability in the absence of cooperativity is given by $P_o = (\lambda/(\lambda+1))^4$, which gives $P_o \sim 0.2$ for physiological concentrations of Ca. This result is inconsistent with RyR2 measurements in lipid bilyers which routinely measure $P_o \geq 0.7$ (21, 23). To overcome this limitation, we find that cooperative interactions between subunits is essential. In particular, we find that cooperativity can be tuned to allow the mean closed time to be extremely short ($\tau_c \sim 1ms$) at high Ca, and then be very large at low Ca ($\tau_c \sim 5000ms$), which is consistent with the single channel measurements of Xu and Meissner (23). In effect, cooperativity can improve the sensitivity of the RyR2 to the Ca concentration changes required for signaling, while at the same time increasing the stability of the channel at resting Ca levels. This dual effect substantially improves the capacity of the RyR2 to serve as a Ca sensor, and it is likely an essential component of the architecture of the RyR2 tetramer. However, we note here that cooperativity is only effective providing there is a delicate balance between δ and ϵ. For example, for a fixed ϵ, if δ exceeds a critical value, the energy penalty required to open the channel is so large that the channel cannot respond to the Ca concentration changes required for Ca signaling. Thus, the response time requirements on the RyR2 places constraints on the relative strength of δ and ϵ. Finally, for the case $k_o = 1$, we found that the RyR2 likely cannot serve as an effective Ca sensor. When $k_o = 1$, most RyR2 conformational states allow Ca to pass through. Thus, in order to stabilize the closed state, the energy penalty δ must be made exceedingly large, which prevents the RyR2 from responding to the sub-millisecond Ca concentration changes due to an LCC opening. Thus, our findings indicate that $k_o = 3$ or 4 is likely optimal for stability and response. Furthermore, our analysis suggests that there cannot be a large difference in the relative stability of the closed (δ) and open (ϵ) state. These findings highlight essential structural requirements in order for RyR2 to serve as an effective Ca sensor.

Several experimental groups have studied the RyR2 in lipid bilayers to measure the dependence of P_o on the cytosolic Ca concentration(21, 24). By fitting P_o to a Hill equation, it is possible to explore the degree of cooperativity involved in RyR2 opening. In particular, Mukherjee et al. (21) estimates the Hill coefficient of the RyR2 to be $h = 1.78$, while Laver et al. (32) has reported Hill coefficients in the range $h = 2 - 3$. Analysis of the 4-subunit model, for the case where $\delta = \epsilon$, suggests that $h = 4$ if $\gamma \ll \lambda$, which corresponds to the case where cooperative interactions dominate the energetics of the system. Thus, Hill coefficients in the range $2 \leq h \leq 3$ imply that the strength of cooperative interactions is limited. This result is consistent with our finding that the subunit-subunit interaction strength cannot be too strong as to make the RyR2 unresponsive to rapid changes in Ca. Also, these experimental findings are consistent with our finding that $k_o \geq 1$. In the case $k_o = 1$, the requirement that $h > 1$ requires that $\gamma \ll \lambda$, which corresponds to the case where the interaction energy between subunits dominates the energetics of the system. Once again, this condition is unlikely given the response constraints on the channel. Overall, we can

conclude that Hill coefficients in the range $h = 2 - 3$ are consistent with our findings that cooperativity is essential, but cannot be made so strong as to make the RyR2 unresponsive to physiological changes in Ca.

Balanced cooperative interactions are required for normal spark activation. In this study, we have analyzed how the kinetics of a Ca spark depend on the cooperative interactions between subunits. We found that a cluster of RyR2 channels responds to a rapid increase of Ca in 3 possible ways: (i) The spark fails to ignite, (ii) Ca is released in the form of a Ca spark which lasts for $20 - 100ms$ and then closes, and (iii) a long-lasting spark which does not close. Our main finding in this study is that a normal Ca spark only occurs within a limited region in the $\delta - \epsilon$ parameter space. In particular, we show that increasing the stability of the open state, by increasing the energy penalty ϵ, favors the development of long-lasting sparks. On the other hand, increasing the stability of the closed state, by increasing the energy penalty δ, can prevent spark activation. Thus, a normal Ca spark only occurs within a limited region in parameter space that is bounded by either activation failure or a long-lasting spark. Furthermore, we found that this region shrinks as k_o is decreased, and is non-existent for $k_o = 1$, since we found that all sparks that form in this case are long-lasting. Here, we also point out that the response in parameter space of a RyR2 cluster, shown in Figure 6, is qualitatively similar to the response of a single RyR2 (Figures 2-4). A partial explanation for the observed differences is that RyR2 kinetics in the cell are modulated by an SR load dependence that is not present in the single channel study. In this study we have evaluated the system response at an SR load of $1400\ \mu M$, and we find that the parameter regime exhibiting long-lasting sparks is substantially larger. This indicates that RyR2 clusters, especially at high SR loads, are highly susceptible to long-lasting sparks. Thus, Ca release is likely to be destabilized by even small changes in the stability of the closed and open states.

Our analysis also reveals that the timing of spontaneous Ca sparks is highly sensitive to cooperativity. Thus, small changes in the stability of the closed or open state can have a large effect on the rate of spontaneous Ca sparks in the cell. This higher rate of spontaneous Ca sparks will contribute to the phenomenon of Ca leak, which has been associated with a wide range of diseased states (9-11). This is because numerous signaling cascades in the cell are regulated by Ca concentration, so that an elevated diastolic Ca concentration may have adverse downstream consequences. Spontaneous Ca sparks have also been implicated as a potential mechanism for cardiac arrythmias. In a recent study, Fowler et al. (33) showed that Ca sparks that occur late in the AP can activate the sodium-calcium exchanger and lead to APD prolongation via early-after-depolarization (EAD). A fraction of these late occurring Ca sparks may be due to spontaneous Ca sparks, which will occur with higher probability late in the AP as the SR is refilled. Thus, modulation of RyR2 cooperativity will alter the bi-directional coupling between Ca and voltage during the AP, which will likely induce dangerous EADs.

Hydrogen bond analysis is consistent with the structural constraints on the RyR2. The preceding conclusions find support in a structural analysis of the RyR2 tetramer. In Figure 1B, we show the number of nearest neighbor subunit-

subunit hydrogen bonds (H-bonds) calculated from both the closed state cryo-EM structure (PDB ID: 6JI8) and the open state cryo-EM structure (PDB ID: 6JIY). Taking this estimate of the number of H-bonds at face value, we see that the closed state has a small surplus of hydrogen bonds (H-bonds) between nearest neighbor subunits in comparison to the open state. This implies that the subunit-subunit interaction energy in the closed state is more stable than in the open state. This result is consistent with our finding, shown in Figure 6, that normal Ca sparks occur within a limited range of parameter space where $\delta \gtrsim \epsilon$. Our analysis suggests that the number of subunit-subunit interactions in the closed state conformation needs to be greater in order to ensure that RyR2 flux terminates. Furthermore, our analysis predicts that if there is a large energy difference such that $\delta \gg \epsilon$, the RyR2 cluster will not be responsive to a physiologically relevant current stimulus. Thus, our hydrogen bond analysis is consistent with the main structural requirements for the RyR2 to serve as effective Ca sensor.

Implications on diseased states. It is now established that several arrhythmias, such as catecholaminergic polymorphic ventricular tachycardia (CPVT) and long QT syndrome type 2, may be traced to a point mutation in the RyR2 (34-36). Single cell studies of cardiac cells from mutant animals reveals that these mutations cause aberrant Ca leak from the SR (37, 38). However, the precise molecular mechanism that leads to this increased leak is still not fully understood. In this study we show that Ca leak can be driven by long-lasting sparks, which can be induced by over stabilization of the open state, or alternatively, destabilizing the closed state. Specifically, a mutation that modulates the interaction energy between two closed states ($E[0,0]$), or alternatively, two open states ($E[1,1]$) can drive leak by promoting long-lasting sparks. Alternatively, a mutation can also drive the system to the non-responsive regime which may also induce other dangerous compensatory mechanisms. For example, a loss in signaling between the LCC and the RyR2 will promote an increase of SR Ca in order to compensate for the loss of Ca release. In this case the downstream effect can be destabilizing, since elevated SR Ca load can lead to dangerous Ca waves which are known to be highly arrhythmogenic. Interestingly, there are 63 genetic mutations of RyR2 associated with CPVT and/or LQTS(39). In a recent study, we have found that the majority of these mutations reside at sites which can potentially mediate the interaction energy between subunits(40). In addition, Kimlicka et al. (41) have observed that NH2-terminal disease mutation hotspots cluster at domain-domain interfaces. To explain this, they have hypothesized that mutations that remove subunit-subunit interactions in the closed state lower an energy barrier that facilitates a premature transition to the open state, and the authors have suggested that disruption of domain-domain interactions in this way may be a general disease mechanism in RyR channels(42). These results are consistent with our finding that the stability of Ca release is highly sensitive to cooperativity. However, we stress here that exploring downstream consequences of cooperativity will require extensive model validation at the whole cell level. In particular, changes in single channel properties will activate compensatory mechanisms which change Ca cycling homeostasis. It is these changes that will be critical to understanding disease progression.

Model limitations. An important limitation of this study is that our results rely on a specific computational model of Ca cycling in cardiac myocytes. Therefore, it is necessary to assess if our main results are robust and not model specific. A key result in this study is that we have evaluated the region in parameter space where normal versus long-lasting sparks occur. In this regard, we refer to the work of Song et al. (30) who analyzed the underlying mechanism for long-lasting sparks using a minimal model of a cluster of RyR2 channels. Their analysis showed that long-lasting sparks occurred when the CRU system transitioned from a monostable to a bistable system. In effect, when the RyR2 open probability is increased, or under SR overload conditions, the CRU system can acquire a stable state where the RyR2 cluster does not completely shut. Further analysis showed that the key requirement for the system to possess bistability is simply that the RyR2 open probability must be a nonlinear function of the diastolic Ca concentration. In this current study, this nonlinearity arises from the cooperative interactions between neighboring subunits, which makes the RyR2 open probability a nonlinear function of the diastolic Ca. Thus, the long-lasting sparks analyzed in our study are likely a robust feature of a wide range of CRU models (43) where the RyR2 open probability is a nonlinear function of Ca. Similarly, spontaneous Ca sparks are due to random RyR2 openings that occur at low diastolic Ca and which can raise the local Ca above threshold. This feature is again dependent on the nonlinear relationship between RyR2 open probability and diastolic Ca, and it is observed in a wide range of computational models(44, 45). Thus, while detailed features of the system will depend on model parameters such as the RyR2 cluster size (46), or the magnitude of the Ca flux across the open RyR2 pore, the main qualitative features depend on nonlinear relationships common to all computational models of the RyR2. The new insight in this study is that these nonlinear relationships between the RyR2 and Ca are highly sensitive to the interaction strength between RyR2 subunits.

A second limitation of this study is that we assume that activation of the RyR2 pore is due to Ca binding to a single cytoplasmic Ca regulatory site. This Ca binding site has been confirmed structurally (19), and it is recognized as the dominant Ca activation site. Nevertheless, additional Ca binding sites have also been proposed, including a luminal activation site and an inactivation site, which are not explicitly accounted for in our present model. Determining the effect of each site on Ca activation has proved to be a challenge experimentally, as both sites are active within the same physiological concentration range as the dominant cytoplasmic Ca activation site. For example, different mechanisms have been proposed to explain the effect of the luminal activation site on the cytoplasmic activation site, such as an ion feed-through mechanism or direct conformational changes within the RyR2 (32, 47). Also, our model is minimal since it assumes that a single RyR2 subunit can be in only one of two states. This is a major simplification, since it is likely that a subunit can occupy several intermediate states which may change the interaction with nearest neighbor subunits. However, characterizing the interactions in this case will be challenging, since there will be many more states of the full RyR2 tetramer. Nevertheless, the theoretical framework presented here can be readily extended to account for additional binding sites and intermediate states once more structural information becomes available.

It should also be mentioned that changes to other regulatory factors that fall outside the scope of our model can potentially lead to leaky channels in a diseased state. For example, it is known that FKBP12.6 binding to the RyR2 is a critical component in determining the size of RYR2 clusters(48). It is known that FKBP12.6 is also necessary to stabilize the closed state of the RyR2 and prevent channel leak (49). It seems reasonable that a less stable closed state would alter subunit-subunit contacts within a single RyR2 channel, leading to a disease state as described by our present model. However, in this case, more possibilities exist, as the defect may also affect interactions between neighboring RyR2 channels. Additional studies will be needed to model the full effect of accessory proteins such as FKPB12.6 binding to the RyR2.

Appendix

A. The partition sum

The equilibrium properties of the RyR2 tetramer are governed by the partition sum

$$Z = \sum_{\{\vec{s}\}} \exp(-\beta H[\vec{s}]) \ , \qquad (A1)$$

where $\vec{s}$ denotes a string of subunit states that can be either closed (0) or open (1). Once the partition sum is known, the probability of finding the tetramer in state $\vec{s}$, at equilibrium, is given by $P[\vec{s}] = \exp(-\beta H[\vec{s}])/Z$. To compute the partition sum, it is convenient to introduce the terms

$$q = \exp\left[-\beta E[0]\right] , \qquad (A2)$$

$$p = \exp\left[-\beta E[1]\right], \qquad (A3)$$

where $E[0]$ and $E[1]$ is the energy of the closed and open states respectively, and where subunit interactions are neglected. To account for subunit-subunit interactions, we introduce the terms

$$a = \exp\left[-\beta E[1,1]\right] , \qquad (A4)$$

$$b = \exp\left[-\beta E[0,0]\right] , \qquad (A5)$$

$$c = \exp\left[-\beta E[1,0]\right]. \qquad (A6)$$

The partition sum then reads

$$Z = p^4a^4 + 4qp^3a^2c^2 + 4q^2p^2abc^2 + 2q^2p^2c^4 + 4q^3pb^2c^2 + q^4b^4 \, . \qquad (A7)$$

B. The open probability P_o

The open probability can be computed exactly by enumerating all states with $k \geq k_o$ open channels. To proceed, we introduce the dimensionless quantities

$$\lambda = \frac{p}{q} \ , \qquad (B1)$$

$$\alpha = \frac{a}{b}, \qquad (B2)$$

$$\gamma = \frac{c}{b} \,. \tag{B3}$$

These ratios are given by

$$\lambda = \frac{A_{01}}{k_{10}} \frac{[Ca]}{[Ca] + c_{th}} = \frac{k_{01}}{k_{10}}, \tag{B4}$$

$$\alpha = \exp\big(2(\delta - \epsilon)\big) \,, \tag{B5}$$

$$\gamma = \exp(-2\delta) \,. \tag{B6}$$

The open probability of RyR2 for different k_o is given by:

$$P_o(k_o = 4) = \frac{\alpha^4\lambda^4}{\alpha^4\lambda^4 + 4\alpha^2\gamma^2\lambda^3 + 4\alpha\gamma^2\lambda^2 + 2\gamma^4\lambda^2 + 4\gamma^2\lambda + 1} \,, \tag{B7}$$

$$P_o(k_o = 3) = \frac{\alpha^4\lambda^4 + 4\alpha^2\gamma^2\lambda^3}{\alpha^4\lambda^4 + 4\alpha^2\gamma^2\lambda^3 + 4\alpha\gamma^2\lambda^2 + 2\gamma^4\lambda^2 + 4\gamma^2\lambda + 1} \,, \tag{B8}$$

$$P_o(k_o = 2) = \frac{\alpha^4\lambda^4 + 4\alpha^2\gamma^2\lambda^3 + 4\alpha\gamma^2\lambda^2 + 2\gamma^4\lambda^2}{\alpha^4\lambda^4 + 4\alpha^2\gamma^2\lambda^3 + 4\alpha\gamma^2\lambda^2 + 2\gamma^4\lambda^2 + 4\gamma^2\lambda + 1} \,, \tag{B9}$$

$$P_o(k_o = 1) = \frac{\alpha^4\lambda^4 + 4\alpha^2\gamma^2\lambda^3 + 4\alpha\gamma^2\lambda^2 + 2\gamma^4\lambda^2 + 4\gamma^2\lambda}{\alpha^4\lambda^4 + 4\alpha^2\gamma^2\lambda^3 + 4\alpha\gamma^2\lambda^2 + 2\gamma^4\lambda^2 + 4\gamma^2\lambda + 1} \,. \tag{B10}$$

C. The mean closed time

The mean closed time can be solved analytically for the case $k_o = 4$ and $k_o = 1$. For the case $k_o = 1$, this is simply the waiting time for one of the four closed subunits to transition to the open state. This yields a mean closed time of

$$\tau_c(k_o = 1) = \frac{1}{4k_{01}} \exp(2\delta) \,. \tag{C1}$$

For the case $k_o = 4$, the mean open time is determined by the rate at which one of four open subunits transitions to the closed state, which yields

$$\tau_o(k_o = 4) = \frac{1}{4k_{10}} \exp(2\epsilon) \,. \tag{C2}$$

To find the mean closed time for the case $k_o = 4$, we will use

$$P_o = \frac{\tau_o}{\tau_o + \tau_c} \,, \tag{C3}$$

which gives

$$\tau_c(k_o = 4) = \frac{1}{4k_{10}} \exp(2\epsilon) \left(\frac{1 - P_o}{P_o}\right) \,. \tag{C4}$$

Here, P_o is given by Eq. B7, and we can simplify the expression to

$$\tau_c(k_o = 4) = \frac{1}{4k_{10}}(\exp[8\delta - 6\epsilon]\lambda^{-4} + 4\exp[4\delta - 6\epsilon]\,\lambda^{-3} + 4\exp[2\delta - 4\epsilon]\lambda^{-2} + 2\exp[-6\epsilon]\,\lambda^{-2} + 4\exp[-2\,\epsilon]\lambda^{-1}\,)\ . \quad (C5)$$

In this expression the Ca dependent terms are governed by λ while the interaction energies introduce a prefactor that depends on ϵ and δ. To analyze how the interaction energies modify τ_c, it is useful to consider the case where the λ dependence determines the dominant term in Eq. C5. In the small $[Ca]$ limit, where $[Ca] \ll c_{th}$, the leading order behavior is governed by the λ^{-4} term, which gives

$$\tau_c(k_o = 4) \approx \frac{k_{10}^3}{4A_{01}^4}\left(\frac{c_{th}^4}{[Ca]^4}\right)\exp(8\delta - 6\epsilon)\,. \quad (C6)$$

On the other hand, in the large $[Ca]$ limit, the leading order behavior is governed by the λ^{-1} term which gives

$$\tau_c(k_o = 4) \approx \frac{1}{A_{01}}\exp(-2\epsilon). \quad (C7)$$

However, for large interaction energies, the prefactors in Eq. C5 can dominate the sum. In particular, in the case $\delta \gg \epsilon$, the first 3 terms can be larger than the leading order terms in λ, which do not depend on δ. This occurs when

$$\exp[8\delta - 6\epsilon]\lambda^{-4} + 4\exp[4\delta - 6\epsilon]\,\lambda^{-3} + 4\exp[2\delta - 4\epsilon]\lambda^{-2} > 4\exp[-2\,\epsilon]\lambda^{-1} + 2\exp[-6\epsilon]\,\lambda^{-2}\,. \quad (C8)$$

If we compare the leading order terms in λ, on both sides of the inequality, then we have $4\exp[2\delta - 4\epsilon]\lambda^{-2} > 4\exp[-2\epsilon]\lambda^{-1}$, which yields the condition $\delta > \epsilon + \frac{1}{2}\ln(\lambda)$. For the parameters used in this study, this requirement is $\delta > \epsilon + 0.4$. Thus, for large enough δ, the RyR2 loses the capacity to respond rapidly at high Ca. Note here that as δ increased further, the first and second terms in Eq. C8 will dominate. In that case it is straightforward to compare the dominant term on the left side of the inequality with the largest term on the right side. In each case we find that there is always a critical δ above which the inequality is satisfied. This result shows that if δ is large enough, the mean closed time will increase, and the RyR2 will lose its capacity to respond to rapid changes in Ca.

AUTHOR CONTRIBUTIONS

DG, TL, and YS designed research; performed research; contributed analytic tools; analyzed data and wrote the paper.

DECLARATION OF INTERESTS

The authors declare no competing interests.

References

1. Bers, D. M. 2002. Cardiac excitation-contraction coupling. Nature 415:198-205.
2. Cheng, H., and W. J. Lederer. 2008. Calcium sparks. Physiol Rev 88:1491-1545.
3. Bootman, M. D., and M. J. Berridge. 1995. The elemental principles of calcium signaling. Cell 83:675-678.
4. Santulli, G., D. Lewis, A. des Georges, A. R. Marks, and J. Frank. 2018. Ryanodine receptor structure and function in health and disease. Membrane protein complexes: structure and function:329-352.
5. Gong, D., X. Chi, J. Wei, G. Zhou, G. Huang, L. Zhang, R. Wang, J. Lei, S. Chen, and N. Yan. 2019. Modulation of cardiac ryanodine receptor 2 by calmodulin. Nature 572:347-351.
6. Baddeley, D., I. D. Jayasinghe, L. Lam, S. Rossberger, M. B. Cannell, and C. Soeller. 2009. Optical single-channel resolution imaging of the ryanodine receptor distribution in rat cardiac myocytes. Proceedings of the National Academy of Sciences of the United States of America 106:22275-22280.
7. Soeller, C., and D. Baddeley. 2013. Super-resolution imaging of EC coupling protein distribution in the heart. Journal of molecular and cellular cardiology 58:32-40.
8. Zahradnikova, A., I. Zahradník, I. Györke, and S. Györke. 1999. Rapid activation of the cardiac ryanodine receptor by submillisecond calcium stimuli. The Journal of general physiology 114:787-798.
9. Marks, A. R. 2013. Calcium cycling proteins and heart failure: mechanisms and therapeutics. The Journal of clinical investigation 123:46-52.
10. Dridi, H., A. Kushnir, R. Zalk, Q. Yuan, Z. Melville, and A. R. Marks. 2020. Intracellular calcium leak in heart failure and atrial fibrillation: a unifying mechanism and therapeutic target. Nature Reviews Cardiology 17:732-747.
11. Fauconnier, J., J. Thireau, S. Reiken, C. Cassan, S. Richard, S. Matecki, A. R. Marks, and A. Lacampagne. 2010. Leaky RyR2 trigger ventricular arrhythmias in Duchenne muscular dystrophy. Proceedings of the National Academy of Sciences 107:1559-1564.
12. Stern, M. D., L.-S. Song, H. Cheng, J. S. Sham, H. T. Yang, K. R. Boheler, and E. Ríos. 1999. Local control models of cardiac excitation–contraction coupling: a possible role for allosteric interactions between ryanodine receptors. The Journal of general physiology 113:469-489.
13. Bray, D., and T. Duke. 2004. Conformational spread: the propagation of allosteric states in large multiprotein complexes. Annual review of biophysics and biomolecular structure 33:53.
14. Stern, M. D., L. S. Song, H. Cheng, J. S. Sham, H. T. Yang, K. R. Boheler, and E. Rios. 1999. Local control models of cardiac excitation-contraction coupling. A possible role for allosteric interactions between ryanodine receptors. The Journal of general physiology 113:469-489.

15. Sobie, E. A., K. W. Dilly, J. dos Santos Cruz, W. J. Lederer, and M. S. Jafri. 2002. Termination of cardiac Ca2+ sparks: an investigative mathematical model of calcium-induced calcium release. Biophysical journal 83:59-78.
16. Radermacher, M., T. Wagenknecht, R. Grassucci, J. Frank, M. Inui, C. Chadwick, and S. Fleischer. 1992. Cryo-EM of the native structure of the calcium release channel/ryanodine receptor from sarcoplasmic reticulum. Biophysical journal 61:936-940.
17. Zalk, R., O. B. Clarke, A. Des Georges, R. A. Grassucci, S. Reiken, F. Mancia, W. A. Hendrickson, J. Frank, and A. R. Marks. 2015. Structure of a mammalian ryanodine receptor. Nature 517:44-49.
18. Williams, A. J., N. L. Thomas, and C. H. George. 2018. The ryanodine receptor: advances in structure and organization. Current Opinion in Physiology 1:1-6.
19. des Georges, A., O. B. Clarke, R. Zalk, Q. Yuan, K. J. Condon, R. A. Grassucci, W. A. Hendrickson, A. R. Marks, and J. Frank. 2016. Structural basis for gating and activation of RyR1. Cell 167:145-157. e117.
20. Greene, D. A., and Y. Shiferaw. 2021. Mechanistic link between CaM-RyR2 interactions and the genesis of cardiac arrhythmia. Biophysical journal 120:1469-1482.
21. Mukherjee, S., N. L. Thomas, and A. J. Williams. 2012. A mechanistic description of gating of the human cardiac ryanodine receptor in a regulated minimal environment. Journal of General Physiology 140:139-158.
22. Pettersen, E. F., T. D. Goddard, C. C. Huang, E. C. Meng, G. S. Couch, T. I. Croll, J. H. Morris, and T. E. Ferrin. 2021. UCSF ChimeraX: Structure visualization for researchers, educators, and developers. Protein Science 30:70-82.
23. Xu, L., and G. Meissner. 2004. Mechanism of calmodulin inhibition of cardiac sarcoplasmic reticulum Ca2+ release channel (ryanodine receptor). Biophysical journal 86:797-804.
24. Györke, I., and S. Györke. 1998. Regulation of the cardiac ryanodine receptor channel by luminal Ca2+ involves luminal Ca2+ sensing sites. Biophysical journal 75:2801-2810.
25. Restrepo, J. G., J. N. Weiss, and A. Karma. 2008. Calsequestrin-mediated mechanism for cellular calcium transient alternans. Biophysical journal 95:3767-3789.
26. Qu, Z., A. Garfinkel, J. N. Weiss, and M. Nivala. 2011. Multi-scale modeling in biology: how to bridge the gaps between scales? Progress in biophysics and molecular biology 107:21-31.
27. Stern, M. D., E. Ríos, and V. A. Maltsev. 2013. Life and death of a cardiac calcium spark. Journal of General Physiology 142:257-274.
28. Laver, D. R., C. Kong, M. Imtiaz, and M. B. Cannell. 2013. Termination of calcium-induced calcium release by induction decay: an emergent property of stochastic channel gating and molecular scale architecture. Journal of molecular and cellular cardiology 54:98-100.
29. Groff, J. R., and G. D. Smith. 2008. Calcium-dependent inactivation and the dynamics of calcium puffs and sparks. Journal of theoretical biology 253:483-499.
30. Song, Z., A. Karma, J. N. Weiss, and Z. Qu. 2016. Long-lasting sparks: Multi-metastability and release competition in the calcium release unit network. PLoS computational biology 12:e1004671.
31. Zima, A. V., E. Picht, D. M. Bers, and L. A. Blatter. 2008. Termination of cardiac Ca2+ sparks: role of intra-SR [Ca2+], release flux, and intra-SR Ca2+ diffusion. Circulation research 103:e105-e115.

32. Laver, D. R. 2007. Ca2+ stores regulate ryanodine receptor Ca2+ release channels via luminal and cytosolic Ca2+ sites. Biophysical journal 92:3541-3555.
33. Fowler, E. D., N. Wang, M. Hezzell, G. Chanoit, J. C. Hancox, and M. B. Cannell. 2020. Arrhythmogenic late Ca2+ sparks in failing heart cells and their control by action potential configuration. Proceedings of the National Academy of Sciences 117:2687-2692.
34. Liu, N., B. Colombi, E. V. Raytcheva-Buono, R. Bloise, and S. G. Priori. 2007. Catecholaminergic polymorphic ventricular tachycardia. Herz Kardiovaskuläre Erkrankungen 32:212-217.
35. Terentyev, D., C. M. Rees, W. Li, L. L. Cooper, H. K. Jindal, X. Peng, Y. Lu, R. Terentyeva, K. E. Odening, and J. Daley. 2014. Hyperphosphorylation of RyRs underlies triggered activity in transgenic rabbit model of LQT2 syndrome. Circulation research 115:919-928.
36. Hamilton, S., R. Veress, A. Belevych, and D. Terentyev. 2021. The role of calcium homeostasis remodeling in inherited cardiac arrhythmia syndromes. Pflügers Archiv-European Journal of Physiology 473:377-387.
37. Chelu, M., and X. Wehrens. 2007. Sarcoplasmic reticulum calcium leak and cardiac arrhythmias. Biochemical Society Transactions 35:952-956.
38. Lehnart, S. E., C. Terrenoire, S. Reiken, X. H. Wehrens, L.-S. Song, E. J. Tillman, S. Mancarella, J. Coromilas, W. Lederer, and R. S. Kass. 2006. Stabilization of cardiac ryanodine receptor prevents intracellular calcium leak and arrhythmias. Proceedings of the National Academy of Sciences 103:7906-7910.
39. Medeiros-Domingo, A., Z. A. Bhuiyan, D. J. Tester, N. Hofman, H. Bikker, J. P. van Tintelen, M. M. Mannens, A. A. Wilde, and M. J. Ackerman. 2009. The RYR2-encoded ryanodine receptor/calcium release channel in patients diagnosed previously with either catecholaminergic polymorphic ventricular tachycardia or genotype negative, exercise-induced long QT syndrome: a comprehensive open reading frame mutational analysis. Journal of the American College of Cardiology 54:2065-2074.
40. D'Artagnan Greene, M. B., Tyler Luchko, Yohannes Shiferaw. 2022. Molecular dynamics simulations of the cardiac ryanodine receptor type 2 (RyR2) gating mechanism.
41. Kimlicka, L., K. Lau, C.-C. Tung, and F. Van Petegem. 2013. Disease mutations in the ryanodine receptor N-terminal region couple to a mobile intersubunit interface. Nature communications 4:1-10.
42. Woll, K. A., and F. Van Petegem. 2022. Calcium-release channels: structure and function of IP3 receptors and ryanodine receptors. Physiological Reviews 102:209-268.
43. Sobie, E. A., K. W. Dilly, J. dos Santos Cruz, W. J. Lederer, and M. S. Jafri. 2002. Termination of cardiac Ca(2+) sparks: an investigative mathematical model of calcium-induced calcium release. Biophysical journal 83:59-78.
44. Colman, M. A. 2019. Arrhythmia mechanisms and spontaneous calcium release: Bi-directional coupling between re-entrant and focal excitation. PLoS computational biology 15:e1007260.
45. Li, P., W. Wei, X. Cai, C. Soeller, M. B. Cannell, and A. V. Holden. 2010. Computational modelling of the initiation and development of spontaneous intracellular Ca2+ waves in ventricular myocytes. Philosophical Transactions of the Royal Society A: Mathematical, Physical and Engineering Sciences 368:3953-3965.

46. Xie, Y., Y. Yang, S. Galice, D. M. Bers, and D. Sato. 2019. Size matters: ryanodine receptor cluster size heterogeneity potentiates calcium waves. Biophysical journal 116:530-539.
47. Fill, M., and D. Gillespie. 2018. Ryanodine receptor open times are determined in the closed state. Biophysical journal 115:1160-1165.
48. Asghari, P., D. R. Scriven, M. Ng, P. Panwar, K. C. Chou, F. van Petegem, and E. D. Moore. 2020. Cardiac ryanodine receptor distribution is dynamic and changed by auxiliary proteins and post-translational modification. Elife 9:e51602.
49. Dridi, H., A. Kushnir, R. Zalk, Q. Yuan, Z. Melville, and A. R. Marks. 2020. Intracellular calcium leak: a unifying mechanism and therapeutic target for heart failure and atrial fibrillation. Nature reviews. Cardiology 17:732.

Figure captions

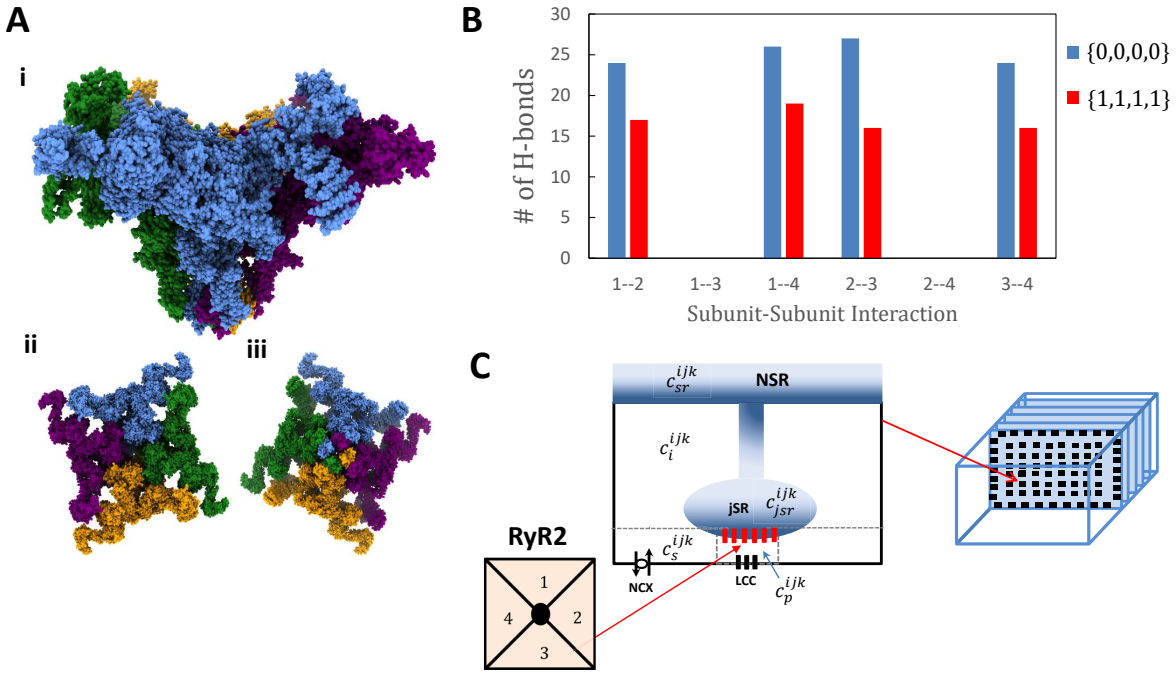

Figure 1. The cryo-EM structure of the closed state of the RyR2 channel is shown in (Ai) a side view, (Aii) a top-down view from the cytosolic side of the channel, and (Aiii) a top-down view from the luminal side of the channel. The four different subunits are colored blue, green, orange, and purple so that they can be easily distinguished from each other. This image was produced using UCSF Chimera X 1.4. (B) Calculation of subunit-subunit hydrogen bond (H-bond) interactions in the closed ($\vec{s} = [0,0,0,0]$) and open ($\vec{s} = [1,1,1,1]$) cryo-EM structures of the closed and open RyR2 channels (PDB ID: 6JI8 and 6JIY, respectively). The subunits on the x-axis were numbered 1-4 to correspond with the coloring scheme shown in Figure 1 where 1(blue), 2(green), 3 (orange), and 4 (purple). For the H-bond calculation, we added hydrogens to the cryo-EM structure using Chimera-X, and we increased the distance tolerance for H-bond determination from its default value of 0.40 Å to 1.0 Å and the angle tolerance from 20.0° to 50.0°. (C) Illustration of the 3D cell model. Ca signaling and release occurs within dyadic junctions distributed in the 3D volume of the cell. Dyadic junctions possess a cluster of RyR2s along with LCC and NCX channels. Here, the superscript ijk denotes the coordinates of a CRU in a 3D grid representing the cell.

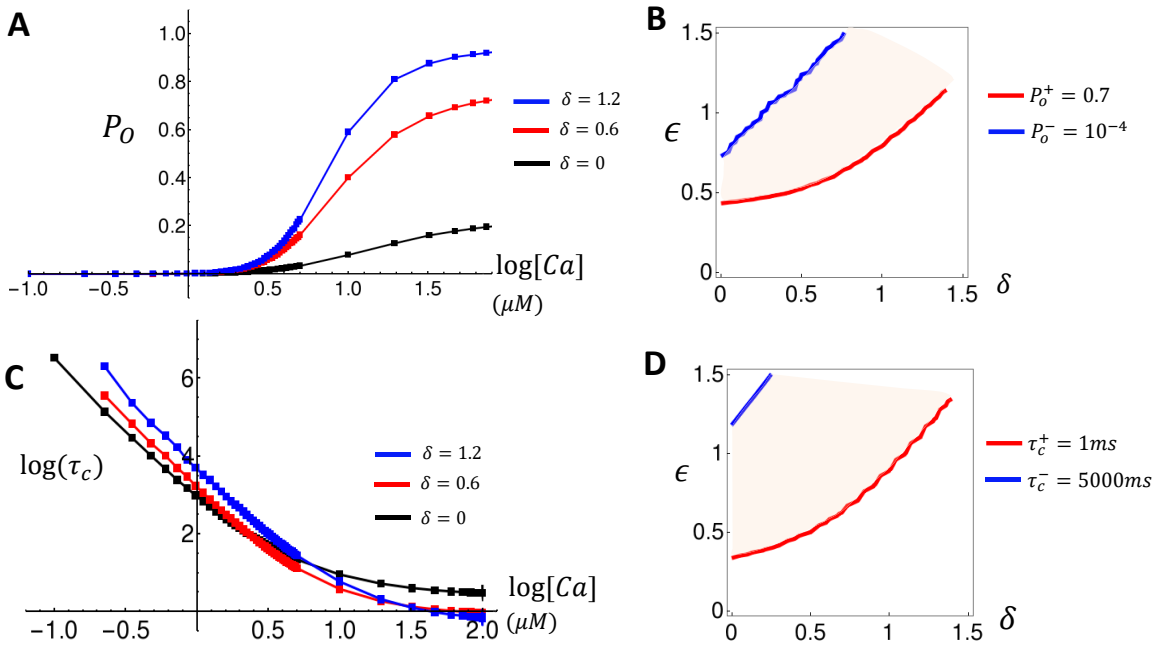

Figure 2. RyR2 channel properties for the case $k_o = 4$. (A) Open probability P_o vs $\log[Ca]$. In this case nearest neighbor interaction energies are symmetric ($\delta = \epsilon$). (B) The region (shaded) in parameter space where RyR2 is both responsive ($P_o^+ \geq 0.7$) and reliably shut ($P_o^- \leq 10^{-4}$). (C) Plot of $\log \tau_c$ as a function of $\log[Ca]$. Interaction energies are taken to be symmetric ($\delta = \epsilon$). (D) The shaded region corresponds to the parameter regime where $\tau_c^+ \leq$ 1 ms and $\tau_c^- \geq 5000$ ms. In these simulations, P_o and τ_c are computed by time evolving a single RyR2 for $t = 10^6\, ms$ using a time step $\Delta t = 0.005\, ms$. In all simulations, quantities are computed by averaging over 500 independent runs. Error bars in Figure A & C are computed using the standard deviation and are smaller than the symbol size.

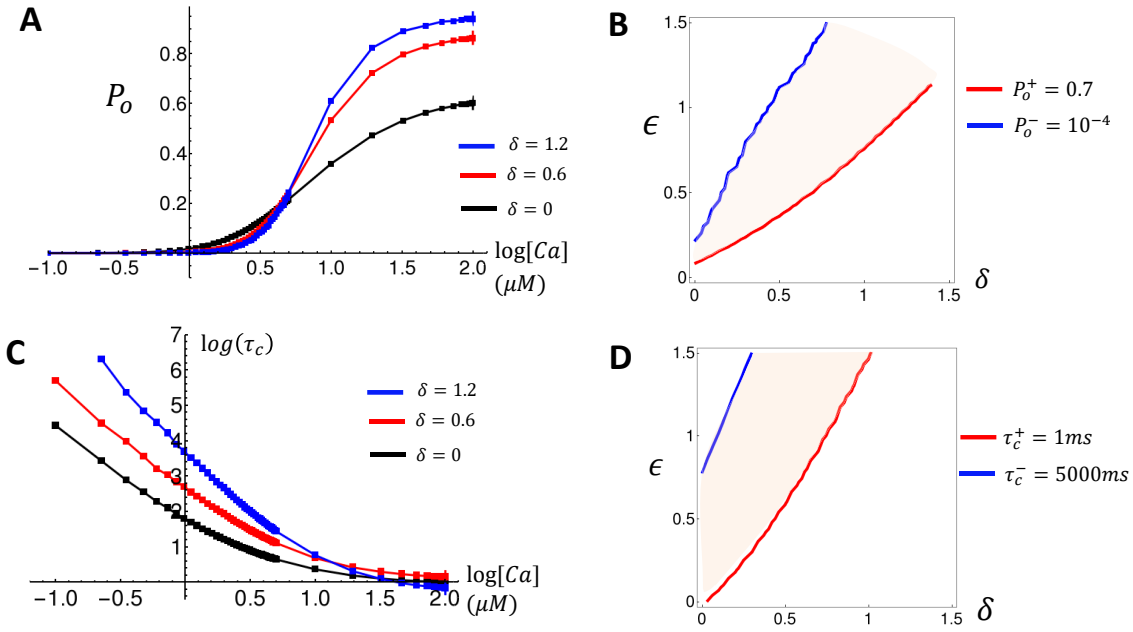

Figure 3. RyR2 channel properties for the case $k_o = 3$. (A) Open probability P_o vs $\log[Ca]$. (B) The parameter regime where $P_o^+ \geq 0.7$ and $P_o^- \leq 10^{-4}$. (C) The mean closed time as a function of $\log[Ca]$ in the case of symmetric interactions ($\delta = \epsilon$). (D) The parameter regime where $\tau_c^+ \leq 1ms$ and $\tau_c^- \geq 5000ms$. For (A) and (C), nearest neighbor interaction energies are chosen to be symmetric ($\delta = \epsilon$), and error bars are smaller than the symbol size.

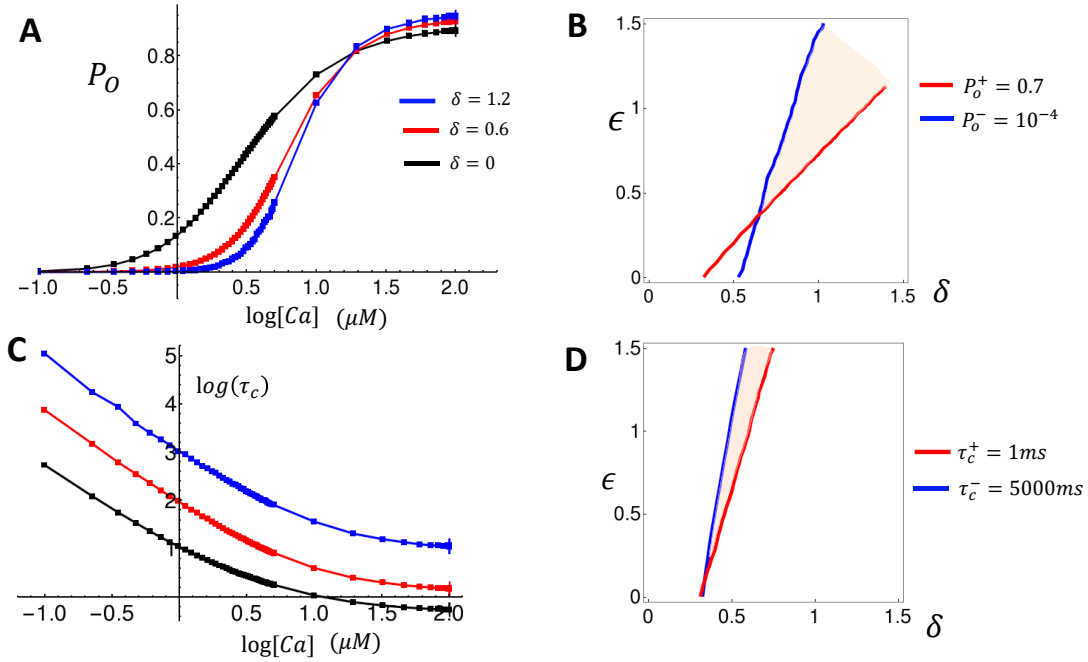

Figure 4. RyR2 channel properties for the case $k_o = 2$. (A) Open probability P_o vs $\log[Ca]$. (B) The parameter regime where $P_o^+ \geq 0.7$ and $P_o^- \leq 10^{-4}$. (C) The mean closed time as a function of $\log[Ca]$. (D) The parameter regime where $\tau_c^+ \leq 1ms$ and $\tau_c^- \geq 5000ms$. For (A) and (C), nearest neighbor interaction energies are chosen to be symmetric ($\delta = \epsilon$), and error bars are smaller than the symbol size.

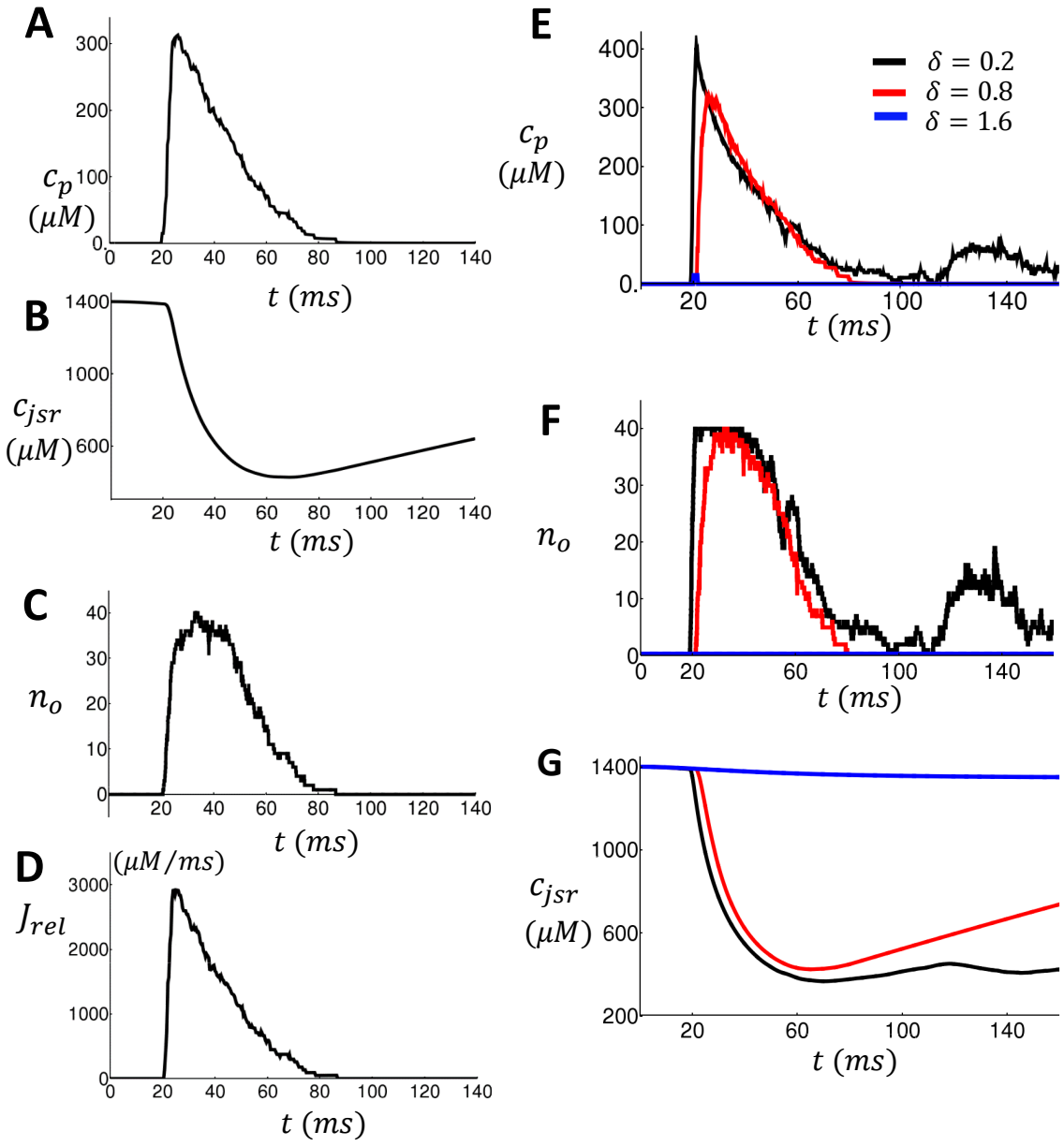

Figure 5. Local fluxes and concentrations during a Ca spark. The local dyadic junction concentration c_p **(A)**, the JSR load c_{jsr} **(B)**, the number of open channels n_o **(C)**, the Ca flux J_{rel} across the RyR2 cluster **(D)** are shown. In this simulation, we have set $k_o = 3$, $N = 40$ and $\delta = \epsilon = 0.8$. A stimulus current of amplitude $150\mu M/ms$ (per unit volume of the dyad) was applied for $1ms$ at time $t = 20ms$. The initial Ca concentration in the dyadic junction is $c_p = 0.1\mu M$, and the SR load is $c_{sr} = 1400\mu M$. To simulate a single dyad, we have set all other RyR2 and LCC conductances to zero. The release flux from the SR is per unit volume of the dyad. In panels **E-G** we repeat the same simulations but fix $\epsilon = 0.8$ and vary δ. Plots shown are: **(E)** Dyadic junction Ca concentration c_p, **(F)** The number of open RyR2 channels n_o, and **(G)** the local JSR load.

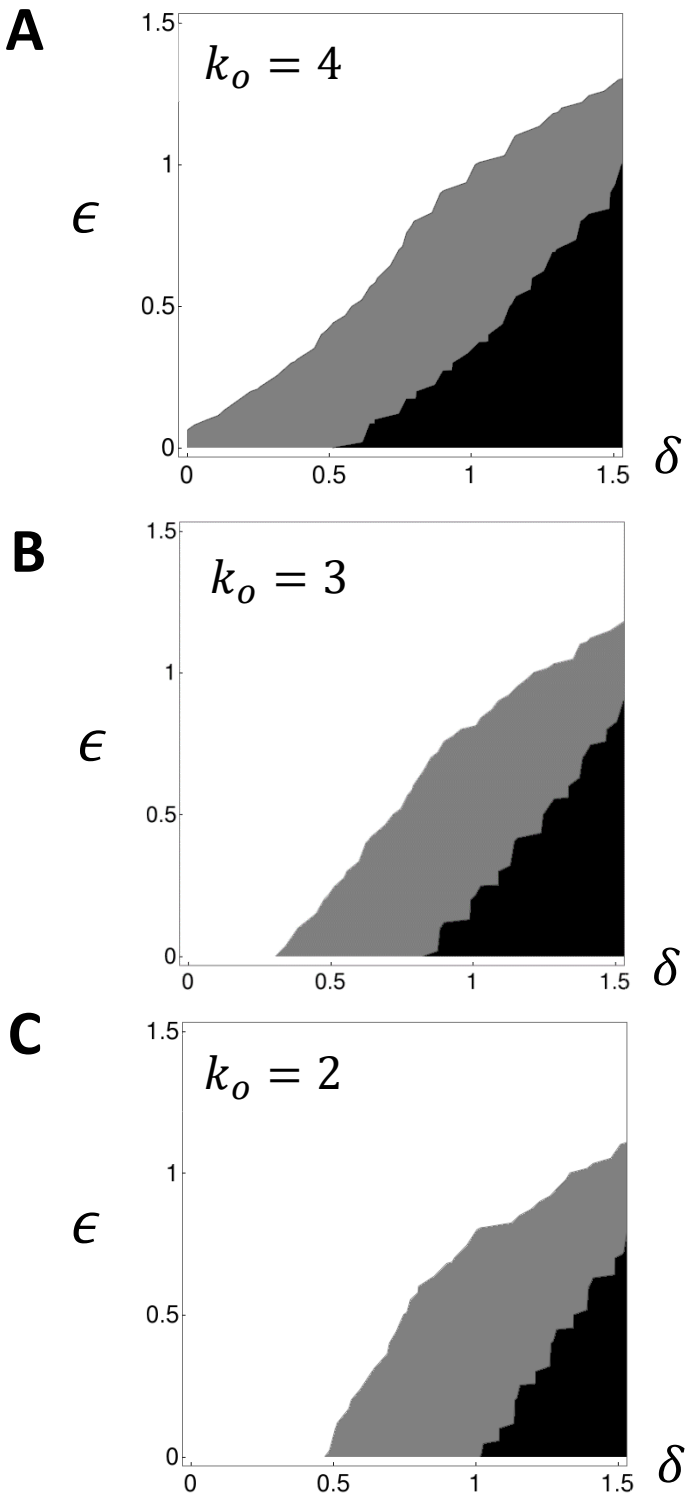

Figure 6. Ca spark life time as a function of subunit interactions for the case (A) $k_o = 4$, (B) $k_o = 3$, and (C) $k_o = 2$. Spark lifetime is computed by averaging over 500 independent runs. The black region denotes failure to trigger, the gray region represents a normal Ca spark, and the white region denotes long-lasting sparks. All initial conditions are the same as in Fig. 5.

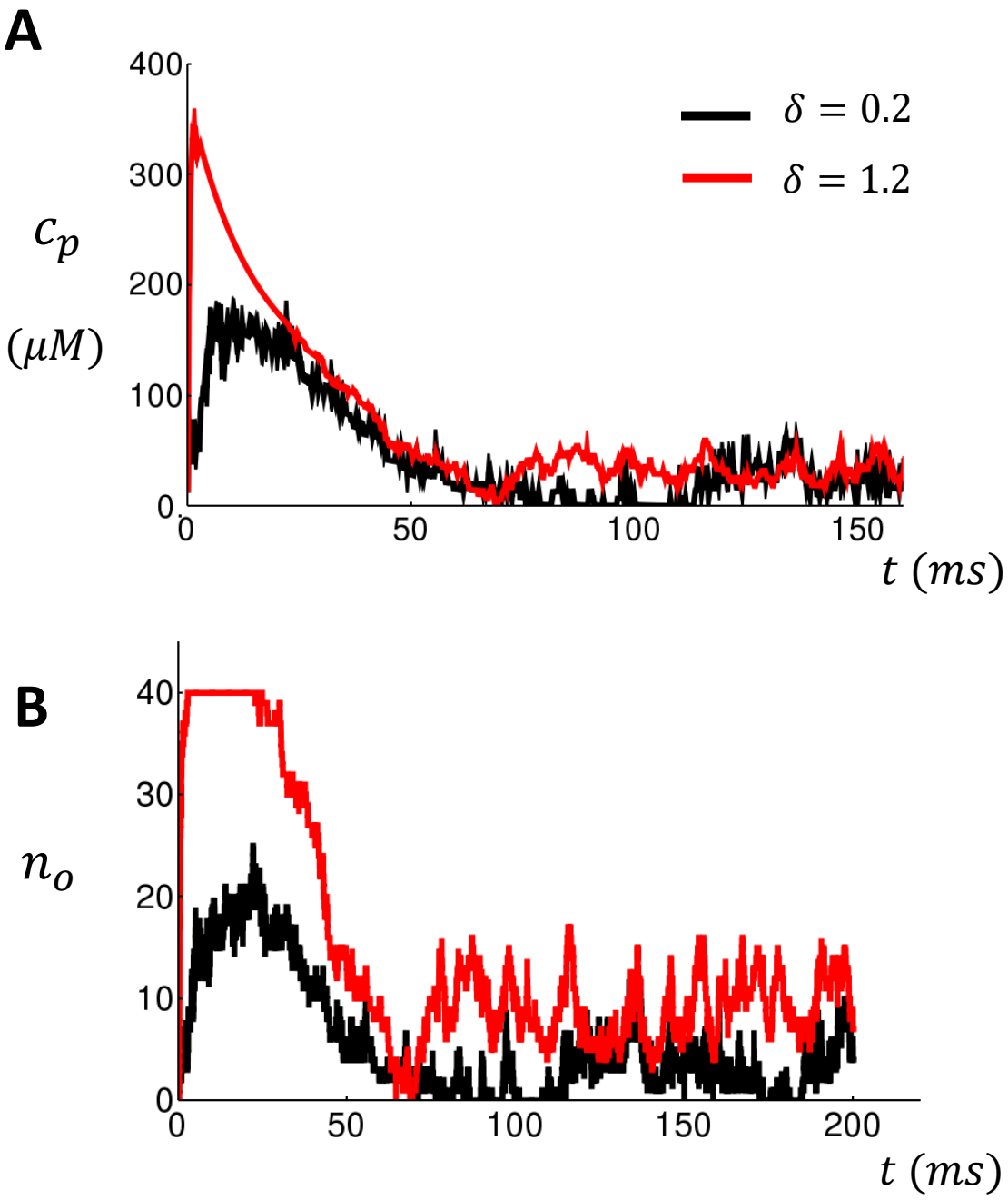

Figure 7. Dyadic junction Ca concentration c_p (A) and number of open RyR2 channels n_o (B) for the case $k_o = 1$. All parameters and initial condition are the same as in Fig. 5. In these simulations we have set $\epsilon = \delta$.

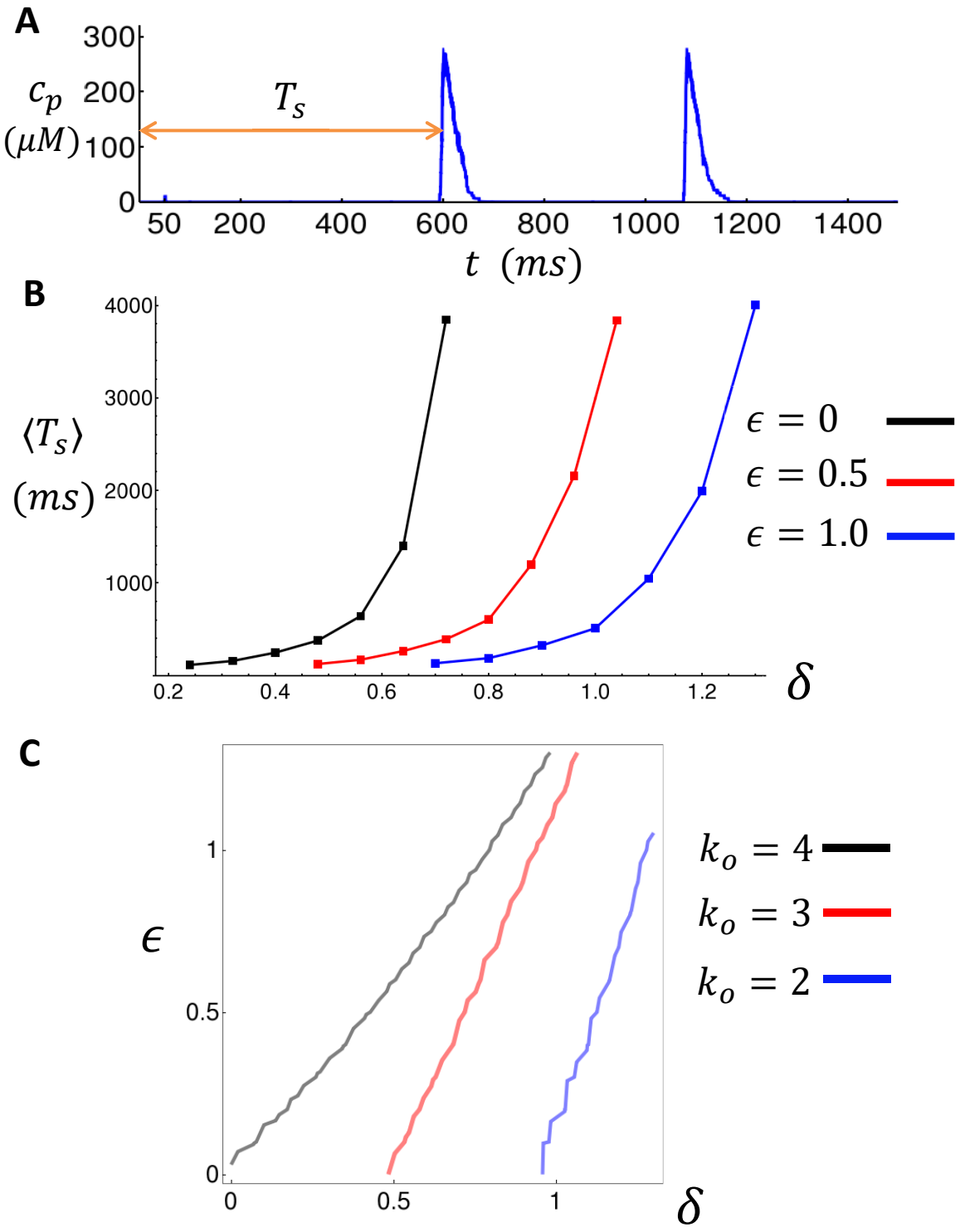

Figure 8. (A) Dyadic Ca concentration for a cluster of size $N = 40$ that was simulated for a long duration of $t = 1500ms$. T_s denotes the waiting time until the first spontaneous Ca spark occurs. Here, we have set $k_o = 3$ and $\delta = \epsilon = 1$. (B) Average waiting time $\langle T_s \rangle$ as a function of δ. The average is taken over 500 independent simulations, and we have set $k_o = 3$. The initial Ca concentration in the dyadic junction is $c_p = 0.1\mu M$ and the SR load is $c_{sr} =$

$1400\mu M$. (C) The line $\langle T_s \rangle = 400ms$ in the $\delta - \epsilon$ parameter space for the cases $k_o = 4, 3$, and 2. Here, the left/right side of the line denotes the region where $\langle T_s \rangle < 400ms$ and $\langle T_s \rangle > 400ms$, respectively.

Table 1

Parameter	Description	Value
A_{01}	Maximum Ca binding rate to a RyR2 subunit	$0.74\ (ms)^{-1}$
c_{th}	Threshold for Ca binding to a RyR2 subunit	$10\mu M$
k_{10}	Transition rate from 1 to 0 of a RyR2 subunit	$0.33\ (ms)^{-1}$